International Journal of Nanomedicine

Dovepress
open access to scientific and medical research

Open Access Full Text Article

ORIGINAL RESEARCH

Effects of silica–gentamicin nanohybrids on osteogenic differentiation of human osteoblast-like SaOS-2 cells

This article was published in the following Dove Press journal:
International Journal of Nanomedicine

Wei He[1]
Dina A Mosselhy[2,3]
Yudong Zheng[1]
Qingling Feng[4]
Xiaoning Li[4]
Xing Yang[4]
Lina Yue[1]
Simo-Pekka Hannula[2]

[1]School of Materials Science and Engineering, University of Science and Technology Beijing, Beijing, People's Republic of China; [2]Department of Chemistry and Materials Science, School of Chemical Engineering, Aalto University, Espoo, Finland; [3]Microbiological Unit, Fish Diseases Department, Animal Health Research Institute, Giza, Egypt; [4]State Key Laboratory of New Ceramics and Fine Processing, School of Materials Science and Engineering, Tsinghua University, Beijing, People's Republic of China

Correspondence: Yudong Zheng
School of Materials Science and Engineering, University of Science and Technology Beijing, No. 30, Xueyuan Road, Beijing 100083, People's Republic of China
Tel +86 10 6233 0802
Fax +86 10 6233 2336
Email zhengyudong@mater.ustb.edu.cn

Qingling Feng
State Key Laboratory of New Ceramics and Fine Processing, School of Materials Science and Engineering, Tsinghua University, Beijing 100084, People's Republic of China
Tel +86 10 6278 2770
Fax +86 10 6277 1160
Email biomater@mail.tsinghua.edu.cn

Introduction: In recent years, there has been an increasing interest in silica (SiO_2) nanoparticles (NPs) as drug delivery systems. This interest is mainly attributed to the ease of their surface functionalization for drug loading. In orthopedic applications, gentamicin-loaded SiO_2 NPs (nanohybrids) are frequently utilized for their prolonged antibacterial effects. Therefore, the possible adverse effects of SiO_2–gentamicin nanohybrids on osteogenesis of bone-related cells should be thoroughly investigated to ensure safe applications.

Materials and methods: The effects of SiO_2–gentamicin nanohybrids on the cell viability and osteogenic differentiation of human osteoblast-like SaOS-2 cells were investigated, together with native SiO_2 NPs and free gentamicin.

Results: The results of Cell Count Kit-8 (CCK-8) assay show that both SiO_2–gentamicin nanohybrids and native SiO_2 NPs reduce cell viability of SaOS-2 cells in a dose-dependent manner. Regarding osteogenesis, SiO_2–gentamicin nanohybrids and native SiO_2 NPs at the concentration range of 31.25–125 μg/mL do not influence the osteogenic differentiation capacity of SaOS-2 cells. At a high concentration (250 μg/mL), both materials induce a lower expression of alkaline phosphatase (ALP) but an enhanced mineralization. Free gentamicin at concentrations of 6.26 and 9.65 μg/mL does not significantly influence the cell viability and osteogenic differentiation capacity of SaOS-2 cells.

Conclusions: The results of this study suggest that both SiO_2–gentamicin nanohybrids and SiO_2 NPs show cytotoxic effects to SaOS-2 cells. Further investigation on the effects of SiO_2–gentamicin nanohybrids on the behaviors of stem cells or other regular osteoblasts should be conducted to make a full evaluation of the safety of SiO_2–gentamicin nanohybrids in orthopedic applications.

Keywords: SiO_2 NPs, gentamicin, cytotoxicity, ALP activity, mineralization

Introduction

With the recent progress of nanotechnology in biomedical fields, the use of nanomaterials has received much attention, most markedly in drug delivery, in vivo imaging, and cancer theranostics. Silica nanomaterial is ranked in the top five frequently used nanomaterials in nanotech-based consumer products.[1] Silica (SiO_2) nanoparticles (NPs) have been extensively applied in medical diagnostics, drug delivery, gene therapy, detection of biomolecules, photodynamic therapy, and bioimaging.[2–4] The ease of surface functionalization of SiO_2 NPs for drug loading allows for identifying them as promising carriers for the controlled drug delivery.[5] In orthopedics, SiO_2 NPs encapsulated with antibiotics were frequently used to avoid infections in surgery. Gentamicin has been one of the most widely used antibiotics in orthopedics and an ideal antibiotic for the treatment of osteomyelitis.[6] Previous studies have attempted

submit your manuscript | www.dovepress.com
Dovepress
http://dx.doi.org/10.2147/IJN.S147849

to develop mesoporous SiO_2 NPs–poly(lactide-*co*-glycolide) (PLGA) composites and showed that the released gentamicin from the mesoporous SiO_2 lasted for 4 or 5 weeks, suggesting that PLGA/mesoporous SiO_2 scaffolds were potential drug delivery materials for bone replacement.[7,8]

However, the effects of the gentamicin-loaded SiO_2 NPs on proliferation and osteogenesis of bone-related cells, which are of major importance for their usage in orthopedics, have not been reported yet. SiO_2–gentamicin nanohybrids consist of two compositions, SiO_2 NPs and gentamicin, both of which contribute to the effects on the cell behavior. There have been some reports on the sole effects of native SiO_2 NPs or gentamicin on cell viability and osteogenesis. Conflicting results regarding the cytocompatibility of native SiO_2 NPs have been reported. SiO_2 NPs could be cytotoxic in different cell lines, including human HepG2 hepatoma cells,[9] human endothelial cells,[10] human alveolar epithelial cells (A549),[11] and NIH/3T3 fibroblasts.[11] Meanwhile, other studies have shown that SiO_2 NPs did not significantly influence the cell viability of human and mouse bone marrow mesenchymal stem cells (BMSCs),[12,13] MC3T3-E1 cells[13] and human umbilical vein endothelial cells (HUVECs)[13] even at a high concentration of 1 mg/mL. With regard to osteogenesis, several studies have indicated that SiO_2 NPs could promote differentiation and mineralization of osteoclasts[13–15] and BMSCs.[12,13,16] However, Huang et al[17,18] have found that SiO_2 NPs at concentrations of 4–200 μg/mL had no effects on the osteogenic differentiation of human BMSCs. These aforementioned studies have shown that the effects of SiO_2 NPs on cell proliferation and differentiation depend on the experimental conditions. The size, morphology, and concentration of the NPs and the incubation time were possible factors influencing the results. Regarding gentamicin, few studies have reported its effect on the viability and osteogenesis of bone-related cells. Ince et al[19] have demonstrated that gentamicin at high concentrations (12.5–800 μg/mL) reduced cell viability and alkaline phosphatase (ALP) activity of pre-osteoblast C2C12 cells and consequently could be detrimental to bone healing and repair. Kagiwada et al[20] have indicated that 200 μg/mL of gentamicin significantly inhibited the cell growth and differentiation capacity of human BMSCs, while 20 μg/mL of gentamicin well supported cell proliferation and differentiation capability. The two aforementioned studies have suggested that the concentration of gentamicin was a key factor in determining its effects.

In our previous study, we have prepared SiO_2–gentamicin nanohybrids and investigated their antibacterial performance.[21] The results have shown that the initial fast release of gentamicin from the nanohybrids fits the need for high concentrations of antibiotics after orthopedic surgery and the extended release of gentamicin justified the ideal antibacterial administration of the nanohybrids in bone applications.[21] In order to assess the implications of the developed materials in practical application, we have conducted further work on the effects of SiO_2–gentamicin nanohybrids on cell viability and osteogenesis of human osteoblast-like SaOS-2 cells in the present study. To the best of our knowledge, this is the first report to investigate the effects of SiO_2–gentamicin nanohybrids on the osteogenic differentiation of bone-related cells. Understanding the effects of SiO_2–gentamicin nanohybrids on osteogenic differentiation of osteoblasts provides important insights on their potential usage in orthopedics. Furthermore, our work is designed to elucidate the influence of SiO_2–gentamicin nanohybrids in comparison with native SiO_2 NPs and free gentamicin on osteogenesis. The results obtained from this investigation provide a better knowledge, addressing the feasibility of using SiO_2–gentamicin nanohybrids in orthopedics.

Materials and methods

Preparation and characterization of the SiO_2–gentamicin nanohybrids and native SiO_2 NPs

SiO_2–gentamicin nanohybrids were prepared by adapting the base-catalyzed precipitation method used by Corrêa et al.[22] Briefly, 500 mg of gentamicin sulfate (Sigma-Aldrich Co., St Louis, MO, USA) was dissolved in 10 mL of tetraethyl orthosilicate (TEOS; ≥99.0%, Sigma-Aldrich, St Louis, MO, USA) with stirring. Then, 20 mL of ammonium hydroxide (28%–30%; Sigma-Aldrich Co.) was dropwise added to the solution. The mixture was stirred for 20 min at room temperature until precipitation. The resultant precipitate was dried overnight at room temperature and then ground. The native SiO_2 NPs were prepared with the same abovementioned method without the addition of gentamicin sulfate.

The surface morphology of the prepared materials was examined by a scanning electron microscope (SEM; MERLIN Compact; Carl Zeiss Meditec AG, Jena, Germany, and S-4700 SEM; Hitachi Ltd., Tokyo, Japan). The size of the prepared NPs was visualized by transmission electron microscope (TEM; H-7650B; Hitachi Ltd.), and the size distributions of the NPs on the obtained TEM images were analyzed by the program Nano Measurer 1.2.5. The Fourier-transform infrared (FTIR) spectra of the SiO_2–gentamicin nanohybrids, native SiO_2 NPs, and gentamicin were recorded on a TENSOR II FTIR spectrometer (Optik GmbH, Ettlingen, Germany) in the attenuated total reflection (ATR) mode, with a resolution of 4 cm^{-1} and a scan range of 4,000–400 cm^{-1}.

Thermogravimetric analysis (TGA) of the SiO_2–gentamicin nanohybrids and native SiO_2 NPs was performed on a Q600 SDT thermal analyzer (TA Instruments, New Castle, DE, USA). The analysis was conducted from 50°C to 500°C with a heating rate of 10°C/min under a nitrogen atmosphere (flow rate of 20 mL/min).

Cell culture and exposure to NPs

Human osteogenic sarcoma cells (SaOS-2; purchased from China Infrastructure of Cell Line Resources) were used in the present study. For expansion, the cells were cultured in a normal culture medium consisting of McCoy's medium (Thermo Fisher Scientific, Waltham, MA, USA), supplemented with 15% fetal bovine serum (FBS; Thermo Fisher Scientific) and 1% penicillin/streptomycin. The medium was changed every 2 days. To induce osteogenesis, cells were incubated in the osteogenic induction medium (the normal culture medium containing 10^{-7} M dexamethasone, 10 mM β-glycerophosphate disodium, and 50 μg/mL ascorbic acid) and the medium was refreshed every 3 days. The cells were kept in a 5% CO_2 humidified incubator at 37°C.

Before experiments, the NPs were exposed to ^{60}Co irradiation at a dose of 10 kGy for sterilization. The cells were allowed to adhere for 24 h before incubation with the nanohybrids. SiO_2–gentamicin nanohybrids were first suspended in the cell culture medium to a concentration of 1 mg/mL and ultrasonically vibrated for 1 h. It is expedient to conduct the ultrasonication in the cell culture medium for 1 h, owing to the virtue of FBS as a promising candidate in mammalian cell culture studies, stabilizing the NPs by sonication.[23] Then, the medium containing SiO_2–gentamicin nanohybrids was diluted to the required concentrations in the cell culture medium and added to the cells. In this experiment, four different concentrations, namely, 31.25, 62.5, 125, and 250 μg/mL, were chosen to treat the cells. After incubation for 72 h, the medium was changed to the fresh one without the nanohybrids. To further elucidate the effects of native SiO_2 NPs and free gentamicin on the osteogenic differentiation of SaOS-2 cells, we have set up four more groups, including native SiO_2 NPs at concentrations of 62.5 and 250 μg/mL and gentamicin at 6.26 and 9.65 μg/mL in the cell culture medium. The SiO_2 NPs were added to the cells in the same way as the SiO_2–gentamicin nanohybrids. Regarding the free gentamicin, the cells were exposed to gentamicin during the whole incubation. The cells incubated in medium with neither NPs nor gentamicin were used as blank control. The concentrations of gentamicin were determined according to our previous work.[21]

Cell viability and proliferation

The cells were seeded in the 96-well plates (Coring Incorporated, Corning, NY, USA) at a density of 2.0×10^4 cells/cm^2 and allowed to attach for 24 h. Then, the cells were treated with the NPs suspended in the cell culture medium for 72 h or gentamicin during the whole incubation period. Cell Count Kit-8 (CCK-8) (Dojindo, Kumamoto, Japan) was used to test the viability of cells cultured in both the normal culture medium (on days 1, 3 and 5 after treatment with NPs or gentamicin) and the osteogenic induction medium (on days 7 and 14 after induction) as detailed in a previous study.[24] Briefly, 10 μL of CCK-8 in 100 μL of the medium was added to the cells in each well and incubated for 1 h at 37°C. Afterward, 100 μL of the solution was transferred to a new 96-well plate and the absorbance at 450 nm was quantified by a multimode plate reader (EnSpire; PerkinElmer Inc., Waltham, MA, USA). The experiments were performed in triplicate.

Moreover, cells in the normal culture medium after treatment with NPs and gentamicin for 1, 3, and 5 days were stained with Calcein-AM (Dojindo) to evaluate the cell proliferation. The cells were first rinsed with phosphate-buffered saline (PBS; Coring Incorporated) three times and then stained with the 2 μM Calcein-AM working solution at 37°C for 15 min. Subsequently, the stained cells were observed by an inverted fluorescence microscope (Leica DFC420C; Leica Microsystems, Wetzlar, Germany).

ALP activity

To induce osteogenesis, SaOS-2 cells were first seeded in the 48-well plates (Coring Incorporated) at a density of 2.0×10^4 cells/cm^2 in the normal culture medium. When cells reached 90% confluency, the normal culture medium was changed to osteogenic induction medium containing NPs or gentamicin. The cells were treated with NPs for 72 h or gentamicin during the whole incubation period. After osteogenic induction for 7 days, the cells were washed twice with PBS and then lysed with radioimmunoprecipitation assay (RIPA) lysis buffer (Beyotime, Shanghai, China) for 15 min on ice. The lysate was centrifuged at 12,000 rpm for 10 min, and the supernatant was analyzed by an ALP testing kit (Nanjing Jiancheng Bioengineering Research Institute, Nanjing, China) according to the manufacturer's instructions. Total protein content was determined using the BCA protein assay (Aidlab Biotechnologies Co., Ltd., Beijing, China). The ALP levels were normalized to the total protein content, and the experiments were performed in triplicate.

For qualitative analysis, the cells were washed with PBS and then fixed with 4% (w/v) paraformaldehyde for 30 min.

After fixation, the cells were stained with BCIP/NBT ALP Color Development Kit (Beyotime) and visualized under an inverted optical microscope (Leica DFC420C). Moreover, the plates were photographed using a digital camera (Canon PowerShot SX50 HS; Canon, Tokyo, Japan).

Collagen secretion

The cells were seeded and treated with the same above-described method. After osteogenic induction for 7 days, the collagen in cells was stained with 0.5 mL of 0.1% Sirius Red solution (Beijing Solarbio Science & Technology Co. Ltd., Beijing, China) at room temperature for 18 h. Subsequently, the stained cells were rinsed with distilled water repeatedly and observed by an inverted optical microscope. Moreover, the plates were photographed using a digital camera. To quantify the results of collagen secretion, the stained cells were dissolved by an elution (0.2 M NaOH:methanol =1:1) and the absorbance at 570 nm was measured by a multimode plate reader. The collagen secretion of the cells was normalized to the cell viability detected by CCK-8. The experiments were performed in triplicate.

Expression of type I collagen (COLI), osteopontin (OPN) and osteocalcin (OCN)

The cells were seeded and treated with the same above-described method. Immunofluorescent staining was conducted according to a previous report[25] to evaluate the expression of osteogenic marker proteins, including COLI, OPN (on day 7 after induction), and OCN (on day 14 after induction). Briefly, the cells were washed twice with PBS, fixed with 4% (w/v) paraformaldehyde for 30 min, and then permeabilized with 0.2% Triton X-100 for 5 min. After twice washing with PBS, the cells were further treated with a blocking solution of 10% goat serum at room temperature for 30 min to prevent nonspecific background staining. Thereafter, cells were incubated with rabbit polyclonal antibodies against COLI (ab21285; Abcam, Cambridge, UK), rabbit polyclonal antibodies against OPN (ab8448; Abcam), and mouse monoclonal antibodies against OCN (ab13418; Abcam) at 4°C overnight. Then, the cells were labeled with Alexa Fluor 488-labeled goat anti-rabbit IgG (Beyotime) and Alexa Fluor 594-labeled goat anti-mouse IgG (EarthOx Life Sciences, Millbrae, CA, USA), respectively, at room temperature for 1 h. Cell nuclei were counterstained with 5 μg/mL 4′-6-diamidino-2-phenylindole (DAPI; Sigma-Aldrich Co.) at room temperature for 15 min. Finally, the cells were imaged under a laser scanning confocal microscope (LSCM; LSM 710 META; Carl Zeiss Meditec AG).

Extracellular matrix (ECM) mineralization

The cells were seeded and treated with the same above-described method. On day 14 after osteogenic induction, Alizarin Red S staining was utilized to examine the ECM mineralization by the cells. The cells were washed twice with PBS, fixed with 4% (w/v) paraformaldehyde for 30 min, and then stained with 1% Alizarin Red S (pH at 4.2) for another 30 min at room temperature. Afterward, the cells were frequently washed with distilled water. The images were taken under an inverted optical microscope (Olympus IX81; Olympus Corporation, Tokyo, Japan). Moreover, the plates were photographed using a digital camera. To quantify the results of ECM mineralization, the stain was dissolved in 10% cetylpyridinium chloride in 10 mM sodium phosphate buffer, and the absorbance at 562 nm was measured by a multimode plate reader. The ECM mineralization of the cells was normalized to the cell viability detected by CCK-8. The experiments were performed in triplicate.

Statistical analysis

Statistical analysis of the obtained data was performed using IBM SPSS Statistics 22 (IBM Corporation, Armonk, NY, USA). The values were represented as the mean ± standard deviation (SD). The data were analyzed by one-way analysis of variance (ANOVA) followed by post hoc comparisons with the least significant difference (LSD) method. Values with $p<0.05$ were considered as statistically significant.

Results

Characterization of the SiO_2–gentamicin nanohybrids and native SiO_2 NPs

The morphology of the prepared SiO_2–gentamicin nanohybrids and native SiO_2 NPs was visualized by SEM, as shown in Figure 1. The native SiO_2 NPs (Figure 1A) are quasi-spherical with smooth surfaces. However, the SiO_2–gentamicin nanohybrids (Figure 1B) show surface roughness, verifying the successful loading of gentamicin onto the surfaces of SiO_2 NPs. Moreover, some nanohybrids coalesce into large aggregates. A relationship between the surface roughness of gentamicin-loaded carriers and the antibiotic release has been revealed in the literature. This relationship stems from the fact that rougher surfaces have larger release areas,[26] facilitating the initial fast antibiotic release from the surfaces of carriers for infection prevention in orthopedics.[27] Consequently, the present SEM images indicate the loading of gentamicin on the surface of SiO_2 NPs, which can support the favorable initial antibiotic release, as proven by our previous report.[21] However, there is abundant room for further progress in determining the best reaction

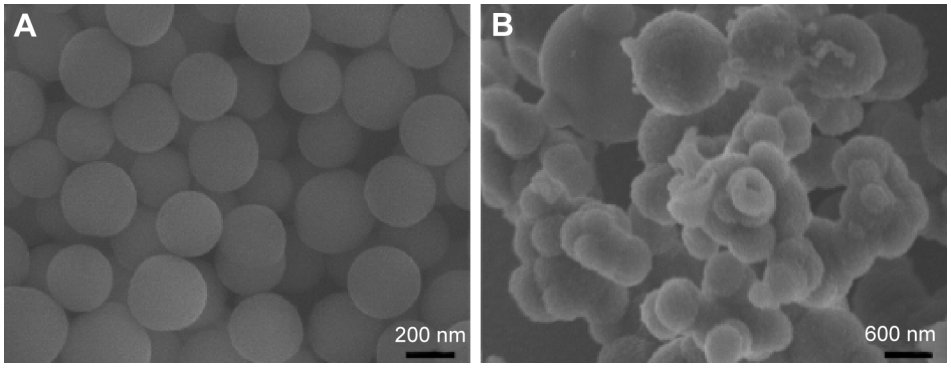

Figure 1 SEM images of the samples.
Notes: (**A**) Native SiO_2 NPs. (**B**) SiO_2–gentamicin nanohybrids.
Abbreviations: SEM, scanning electron microscope; SiO_2, silica; NPs, nanoparticles.

conditions of the nanohybrids, controlling their aggregation and safe applications.

The size and morphology of the native SiO_2 NPs and the SiO_2–gentamicin nanohybrids were further analyzed by TEM, as shown in Figure 2. Most of the native SiO_2 NPs were well dispersed (Figure 2A). The average size of native SiO_2 NPs calculated from the TEM image was 312±26 nm, with a size distribution of 265–405 nm (Figure 2C). The size of the

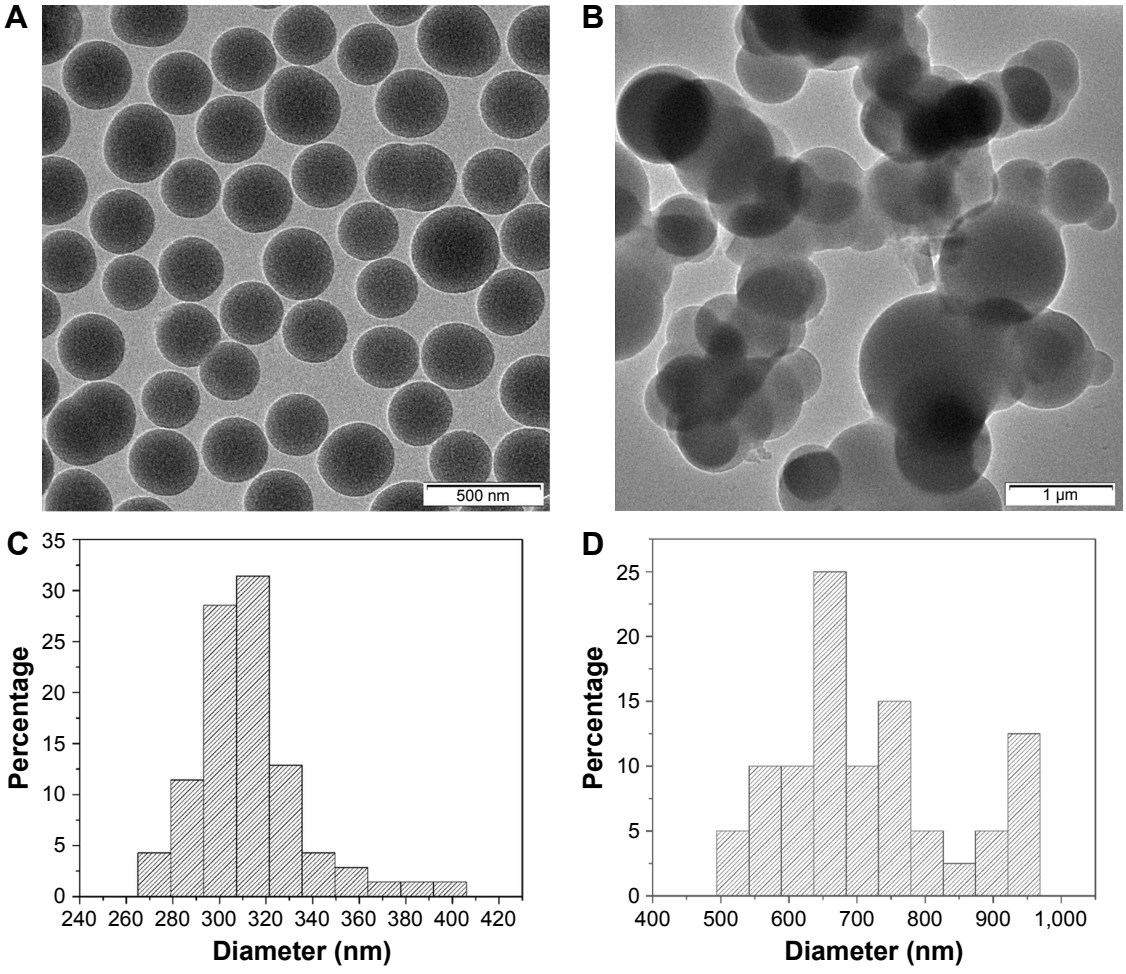

Figure 2 TEM images and size-distribution histograms of the samples.
Notes: TEM images of the (**A**) native SiO_2 NPs and (**B**) SiO_2–gentamicin nanohybrids. Size-distribution histograms of the (**C**) native SiO_2 NPs and (**D**) SiO_2–gentamicin nanohybrids generated from images (**A**) and (**B**), respectively. Most of the native SiO_2 NPs are well dispersed (**A**). The average size of native SiO_2 NPs calculated from the TEM image is 312±26 nm, with a size distribution of 265–405 nm (**C**). The size of the SiO_2–gentamicin nanohybrids increases markedly, compared with the size of the native SiO_2 NPs (**B**). The average size of SiO_2–gentamicin nanohybrids is 719±128 nm, and the size distribution ranges from 495 to 965 nm (**D**).
Abbreviations: TEM, transmission electron microscope; SiO_2, silica; NPs, nanoparticles.

SiO_2–gentamicin nanohybrids increased markedly, compared with the size of the native SiO_2 NPs (Figure 2B). The average size of SiO_2–gentamicin nanohybrids was 719±128 nm, and the size distribution ranged from 495 to 965 nm (Figure 2D). The increase in the size of SiO_2–gentamicin nanohybrids may result from the loading of gentamicin onto the surface of SiO_2 NPs and the encapsulation of some gentamicin within the SiO_2 network. This increase in size is in accord with a recent study,[5] indicating an increase in the size of native SiO_2 NPs from ~160 to ~256 nm after conjugation to gentamicin.

Figure 3A shows the FTIR spectra of the native SiO_2 NPs, free gentamicin, and SiO_2–gentamicin nanohybrids. The native SiO_2 NPs demonstrate peaks at 953 and 800 cm^{-1}, corresponding to symmetric stretching vibrations of the Si–O–Si bond. The sharp peak at 1,053 cm^{-1} corresponds to asymmetric Si–O–Si stretching. A band at 472 cm^{-1} and a broad prominent peak at 3,422 cm^{-1} were detected, associating with the Si–O bond vibration and the Si–OH stretching, respectively. These results are in line with those of previous studies.[21,28,29] The free gentamicin shows a peak at 3,424 cm^{-1} for the stretches of the N–H amino groups[30] and a peak at 618 cm^{-1}, a typical band for gentamicin.[31] The two peaks at 1,529 and 1,629 cm^{-1} were ascribed to the N–H bending vibrations.[32] With regard to the SiO_2–gentamicin nanohybrids, the spectrum shows peaks does 957, 795, and 465 cm^{-1}. The position of the peaks does not notably change from that of the native SiO_2 NPs, but the intensity of the peaks decreases. The peak at 3,441 cm^{-1} likely comprises the same stretches of both the Si–OH and N–H amino groups, but with less intensity. The spectrum of the SiO_2–gentamicin nanohybrids shows new peaks at 618 cm^{-1} and at 1,635 cm^{-1} that were ascribed to native SiO_2 NPs shifted to 1,632 cm^{-1} for the nanohybrids. These new peaks clearly originate from the gentamicin, indicating the successful loading of gentamicin to the native SiO_2 NPs.

TGA results of native SiO_2 NPs and SiO_2–gentamicin nanohybrids are depicted in Figure 3B. The initial weight loss up to 100°C in both samples is induced by the elimination of the absorbed and residual water. The native SiO_2 shows a further weight loss of 6.00% from 100 to 500°C. The SiO_2–gentamicin nanohybrids show a weight loss of 2.16% from 100 to ~220°C and a final weight loss (13.70%) from 220 to 500°C. A temperature of ~220°C can be considered as the beginning of gentamicin decomposition,[33] which continued as the temperature increased. The amount of gentamicin in the SiO_2–gentamicin nanohybrids can be determined by subtracting the mass loss of native SiO_2 NPs from the mass loss of SiO_2–gentamicin nanohybrids, after precluding the weight loss of water in both samples. Therefore, according to the above-described data, gentamicin constitutes 9.86 wt% of the SiO_2–gentamicin nanohybrids. The mass of the dried native SiO_2 NPs and SiO_2–gentamicin nanohybrids was also measured, and the theoretical loading ratio of gentamicin was calculated as 11.27 wt%. This is relevant to the present results of TGA.

Cell viability and proliferation

The possible toxicity of SiO_2–gentamicin nanohybrids, native SiO_2 NPs, and free gentamicin was evaluated on SaOS-2 cells. The viability of cells incubated in the normal culture medium and osteogenic induction medium was determined

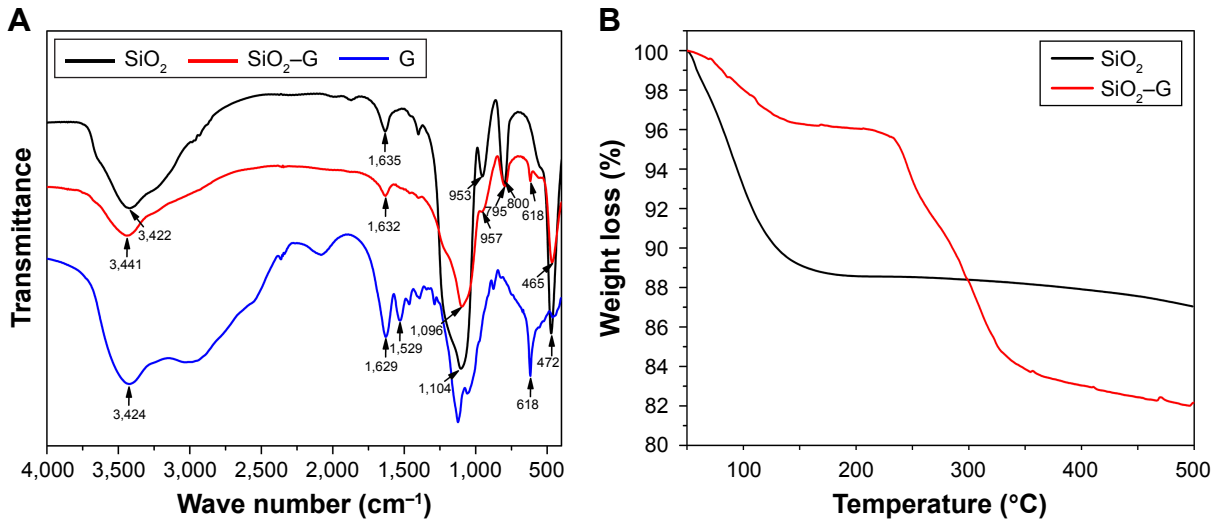

Figure 3 FTIR spectra and TGA of the samples.
Notes: (**A**) FTIR spectra of the native SiO_2 NPs, SiO_2–gentamicin nanohybrids, and free gentamicin. (**B**) TGA of the native SiO_2 NPs and SiO_2–gentamicin nanohybrids.
Abbreviations: FTIR, Fourier-transform infrared; TGA, thermogravimetric analysis; SiO_2, silica; SiO_2–G, SiO_2–gentamicin nanohybrids; NPs, nanoparticles; G, gentamicin.

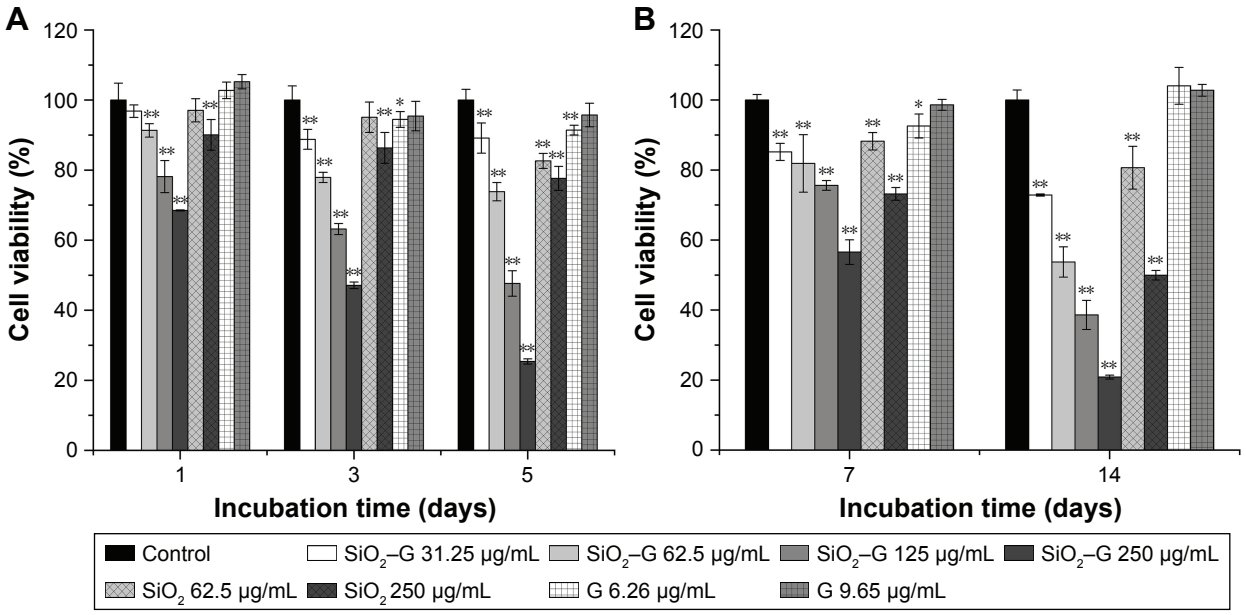

Figure 4 Cell viability detected by CCK-8 assay.
Notes: (**A**) The cells were incubated in the normal medium for 1, 3, and 5 days. (**B**) The cells were incubated in the osteogenic induction medium for 7 and 14 days. The values are expressed as mean ± SD of triplicate experiments. *$p<0.05$ compared with the control group. **$p<0.01$ compared with the control group.
Abbreviations: CCK-8, Cell Count Kit-8; SiO_2, silica; SiO_2–G, SiO_2–gentamicin nanohybrids; G, gentamicin.

after exposing the SaOS-2 cells to the above-described agents. Figure 4A shows the results of cell viability in the normal culture medium. After 1 day, viability of SaOS-2 cells treated with SiO_2–gentamicin nanohybrids decreased to 97%±2%, 91%±2%, 78%±5%, and 68%±0% for concentrations of 31.25, 62.5, 125 and 250 μg/mL, respectively. The viability of cells exposed to SiO_2 NPs at concentrations of 62.5 and 250 μg/mL was 97%±3% and 90%±4%, respectively. However, cells exposed to free gentamicin at concentrations of 6.26 and 9.65 μg/mL show no significant change in viability on day 1. As time progressed, the viability of cells decreased more markedly in SiO_2–gentamicin nanohybrids and native SiO_2 NPs-treated groups. On day 5, the cell viability in 250 μg/mL SiO_2–gentamicin nanohybrid-treated group decreased to 25%±1%, indicating severe cytotoxicity induced by SiO_2–gentamicin nanohybrids. Similar trends were found for the cells incubated in the osteogenic induction medium. As indicated in Figure 4B, both SiO_2–gentamicin nanohybrids and native SiO_2 NPs induce dose- and time-dependent cytotoxicity in SaOS-2 cells, while the tested concentrations of free gentamicin show no obvious cytotoxicity to the cells.

Figure 5 demonstrates the Calcein-AM staining assay, visualizing the proliferation of SaOS-2 cells incubated in the normal culture medium. On day 1, cell numbers decreased for SiO_2–gentamicin nanohybrids and native SiO_2 NP-treated groups as compared to the control group. The trends were more obvious on days 3 and 5; the higher concentration of the NPs tested, the fewer the number of SaOS-2 cells observed. Cell numbers stayed the same for the gentamicin-treated groups. The results are consistent with the cell viability data detected by CCK-8.

Cell differentiation

ALP activity

The ALP activity was assessed qualitatively and quantitatively after 7 days of osteogenic induction. The results are shown in Figure 6. There were no significant differences in the ALP activity between the exposed cells of SiO_2–gentamicin nanohybrids at concentrations of 31.25 and 62.5 μg/mL and the control group. However, the ALP activity significantly decreased as the concentration of SiO_2–gentamicin nanohybrids increased to 125 and 250 μg/mL. The ALP activity expressed by 250 μg/mL exposed cells of SiO_2–gentamicin nanohybrids is less than one-third of the control group. The SiO_2 NP-treated groups demonstrate similar results. At a concentration of 62.5 μg/mL, SiO_2 NPs did not significantly influence the expression of ALP activity. The ALP activity decreased to 38% of the control group as the concentration of SiO_2 NPs increased to 250 μg/mL. The free gentamicin-treated cells show no significant differences in ALP expression compared with the control group.

Collagen secretion

The collagen secretion of SaOS-2 cells after osteogenic induction for 7 days was analyzed by Sirius Red staining.

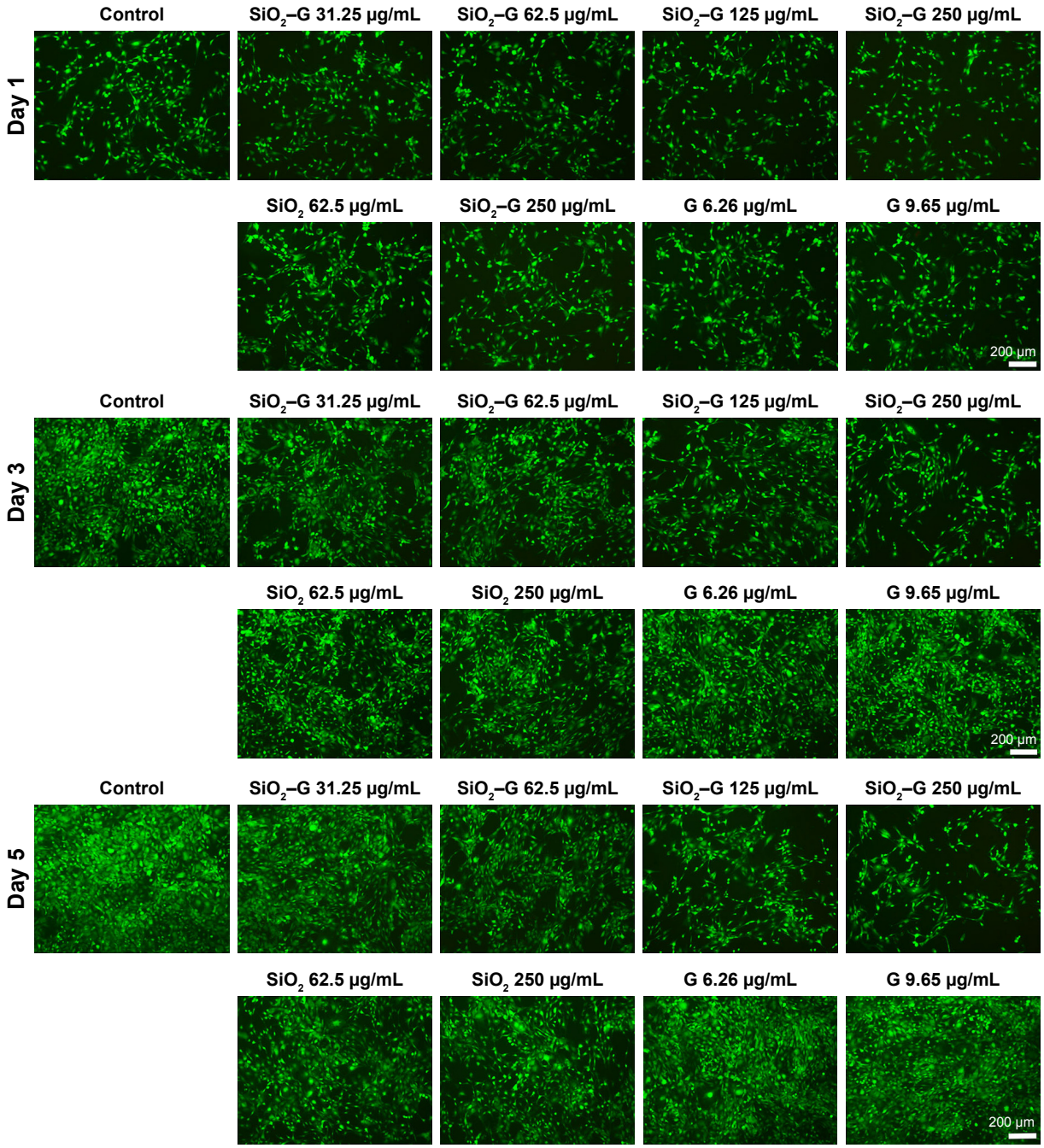

Figure 5 Calcein-AM staining for living cells.
Notes: The cells were incubated with different concentrations of native SiO_2 NPs, SiO_2–gentamicin nanohybrids, and free gentamicin in the normal medium for 1, 3, and 5 days. The images are representative of three independent experiments.
Abbreviations: SiO_2, silica; SiO_2–G, SiO_2–gentamicin nanohybrids; NPs, nanoparticles; G, gentamicin.

The corresponding quantitative analysis is displayed in Figure 7. The collagen secretion of all the experimental groups of SaOS-2 cells cultured for 7 days is not significantly influenced compared with that of the control group, except for the 250 μg/mL SiO_2–gentamicin nanohybrid-exposed group. The secretion of collagen decreased to 90%±7% that of the control group after the exposure of cells to 250 μg/mL SiO_2–gentamicin nanohybrids (Figure 7C).

Expression of COLI, OPN, and OCN

The expression of osteogenesis-related proteins (COLI, OPN, and OCN) was evaluated by immunofluorescent staining. As shown in Figure 8, SaOS-2 cells of all the groups tested are strongly positive for COLI, OPN, and OCN and the cells almost display the same fluorescence intensity for the three kinds of proteins. The group treated with high concentrations of SiO_2–gentamicin nanohybrids or native SiO_2 NPs

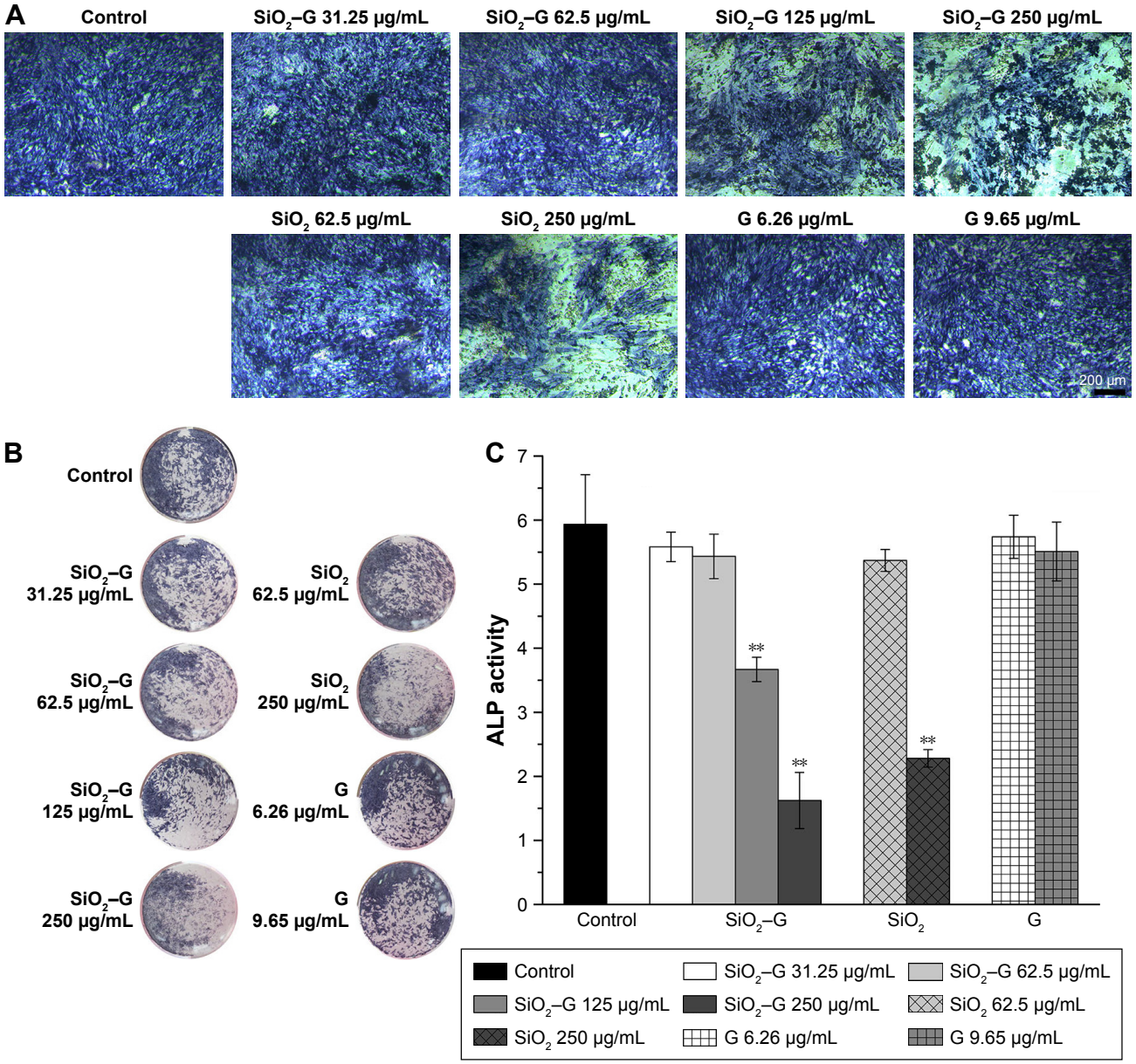

Figure 6 ALP activity of the SaOS-2 cells.
Notes: (**A**) Optical microscopic images and (**B**) macrograph of ALP staining. (**C**) ALP activity of SaOS-2 cells after osteogenic induction for 7 days. Values are expressed as mean ± SD of the triplicate experiments. $^{**}p<0.01$ compared with the control group.
Abbreviations: ALP, alkaline phosphatase; SiO_2, silica; SiO_2–G, SiO_2–gentamicin nanohybrids; G, gentamicin.

shows only a decrease in the cell number. The living cells, however, expressed the same intensity of COLI, OPN, and OCN as the cells of the control group. The results indicate that the exposure to SiO_2–gentamicin nanohybrids, native SiO_2 NPs, and free gentamicin does not influence the expression of COLI, OPN, and OCN of SaOS-2 cells.

ECM mineralization

ECM mineralization of SaOS-2 cells on day 14 after osteogenic induction was evaluated by Alizarin Red S staining. The corresponding quantitative results are depicted in Figure 9. All the exposed groups show almost the same level of ECM mineralization, except for the groups exposed to 250 μg/mL SiO_2–gentamicin nanohybrids and native SiO_2 NPs. The cells formed more mineralized nodules after exposure to 250 μg/mL SiO_2–gentamicin nanohybrids and native SiO_2 NPs (Figure 9A and B). The quantitative results revealed that the SaOS-2 cells exposed to 250 μg/mL SiO_2–gentamicin nanohybrids and native SiO_2 NPs show approximately twofold and fivefold increase in ECM mineralization as compared with those of the control group, respectively (Figure 9C).

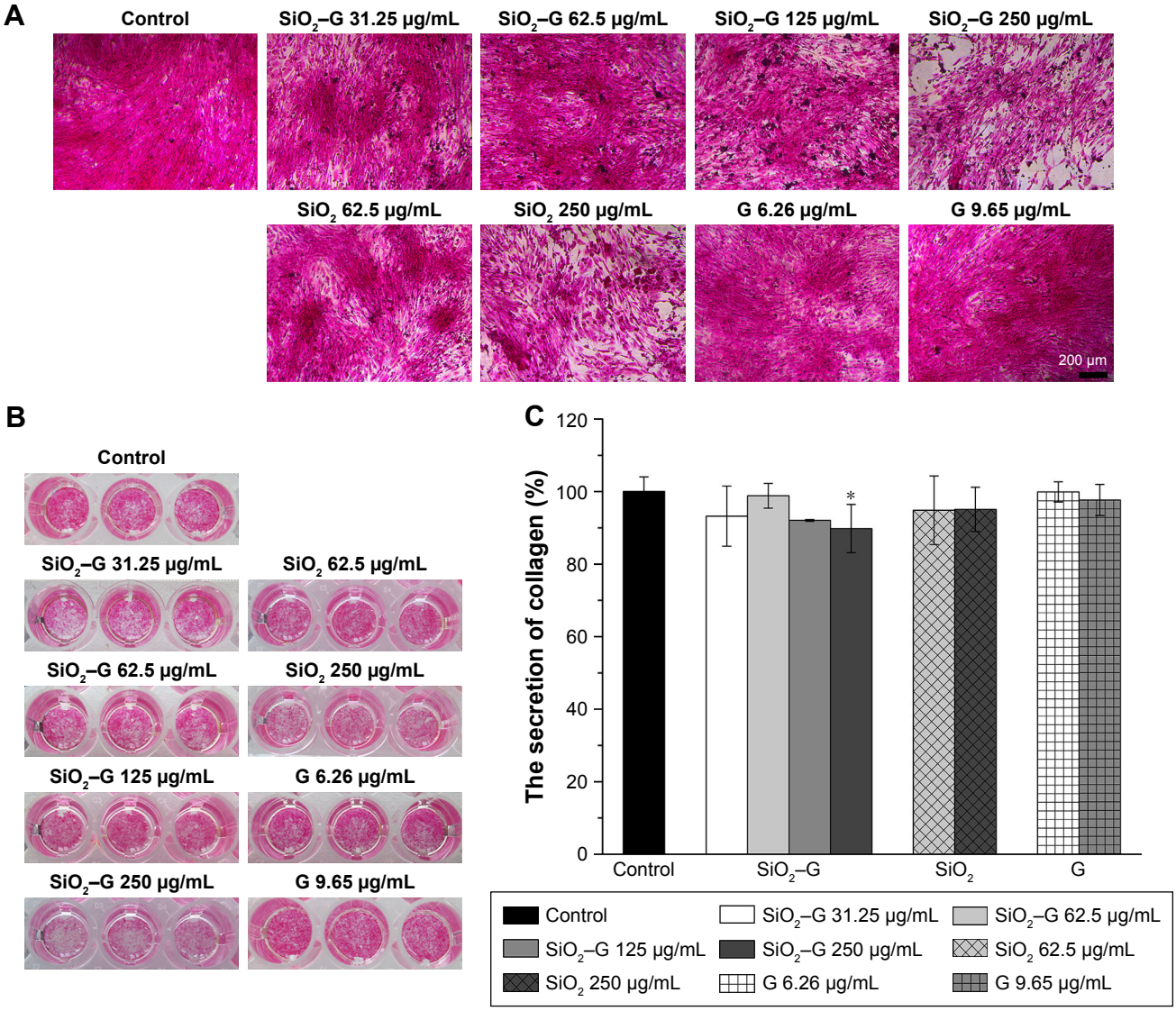

Figure 7 Collagen secretion of the SaOS-2 cells.
Notes: (**A**) Optical microscopic images and (**B**) macrograph of Sirius Red staining for the collagen secretion of cells after osteogenic induction for 7 days. (**C**) The quantitative results of retention of Sirius Red. Data are expressed as mean ± SD (n=3 for each sample). *$p<0.05$ compared with the control group.
Abbreviations: SiO_2, silica; SiO_2–G, SiO_2–gentamicin nanohybrids; G, gentamicin.

Discussion

SiO_2 NPs are used as antibiotic carriers for the extended antibiotic release in orthopedic applications. The minimal negative impact of SiO_2–gentamicin nanohybrids on the viability and osteogenic differentiation capacity of SaOS-2 cells is a prerequisite for using such delivery systems. Our results indicate that both SiO_2–gentamicin nanohybrids and native SiO_2 NPs induce dose- and time-dependent cytotoxicity in SaOS-2 cells (Figures 4 and 5). Moreover, SiO_2–gentamicin nanohybrids are more toxic to the cells than the native SiO_2 NPs at the same concentrations tested. Previous studies have demonstrated that SiO_2 NPs could be cytotoxic in a dose- and time-dependent manner in different cell lines, including human endothelial cells,[10] human alveolar epithelial cells (A549),[11] human cervical cancer cells (HeLa),[34] and human melanoma cells (A375).[35] A conclusion can be drawn from these previous studies that the cytotoxicity of SiO_2 NPs depends not only on concentration and incubation time of NPs but also on other factors, such as size, morphology, and composition of NPs. Therefore, a possible explanation for the present results is that after the loading of gentamicin to SiO_2 NPs, the change in the physicochemical properties of the nanohybrids from the native SiO_2 NPs results in more severe cytotoxicity in SaOS-2 cells. It has been shown that Si

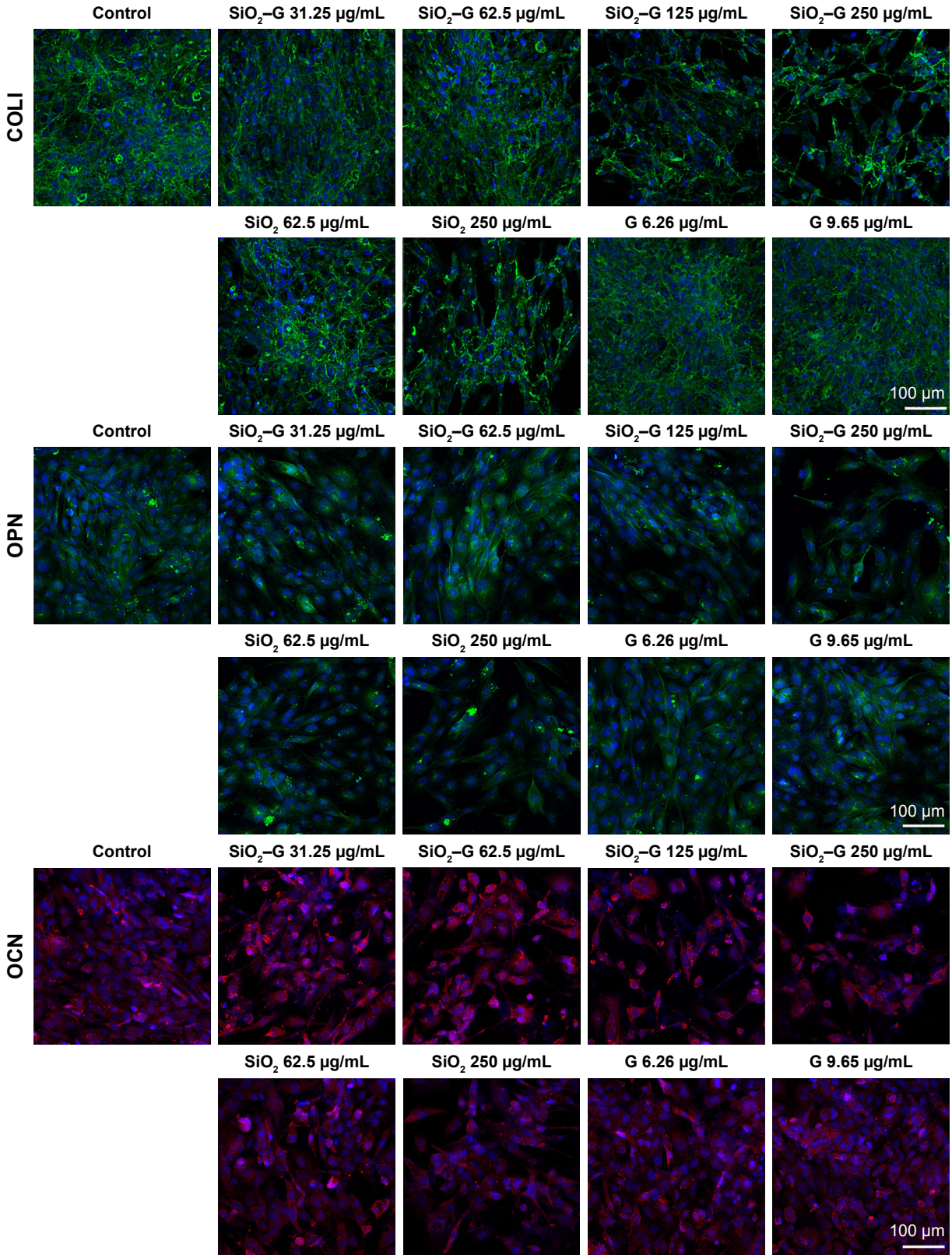

Figure 8 Expression of COLI, OPN, and OCN of the SaOS-2 cells.

Notes: Immunofluorescent staining for COLI, OPN, and OCN. The cells were incubated with different concentrations of native SiO_2 NPs, SiO_2–gentamicin nanohybrids, and free gentamicin in the osteogenic induction medium for 7 days (for COLI and OPN) and 14 days (for OCN). The images are representative of three independent experiments.

Abbreviations: COLI, type I collagen; OPN, osteopontin; OCN, osteocalcin; SiO_2, silica; SiO_2–G, SiO_2–gentamicin nanohybrids; NPs, nanoparticles; G, gentamicin.

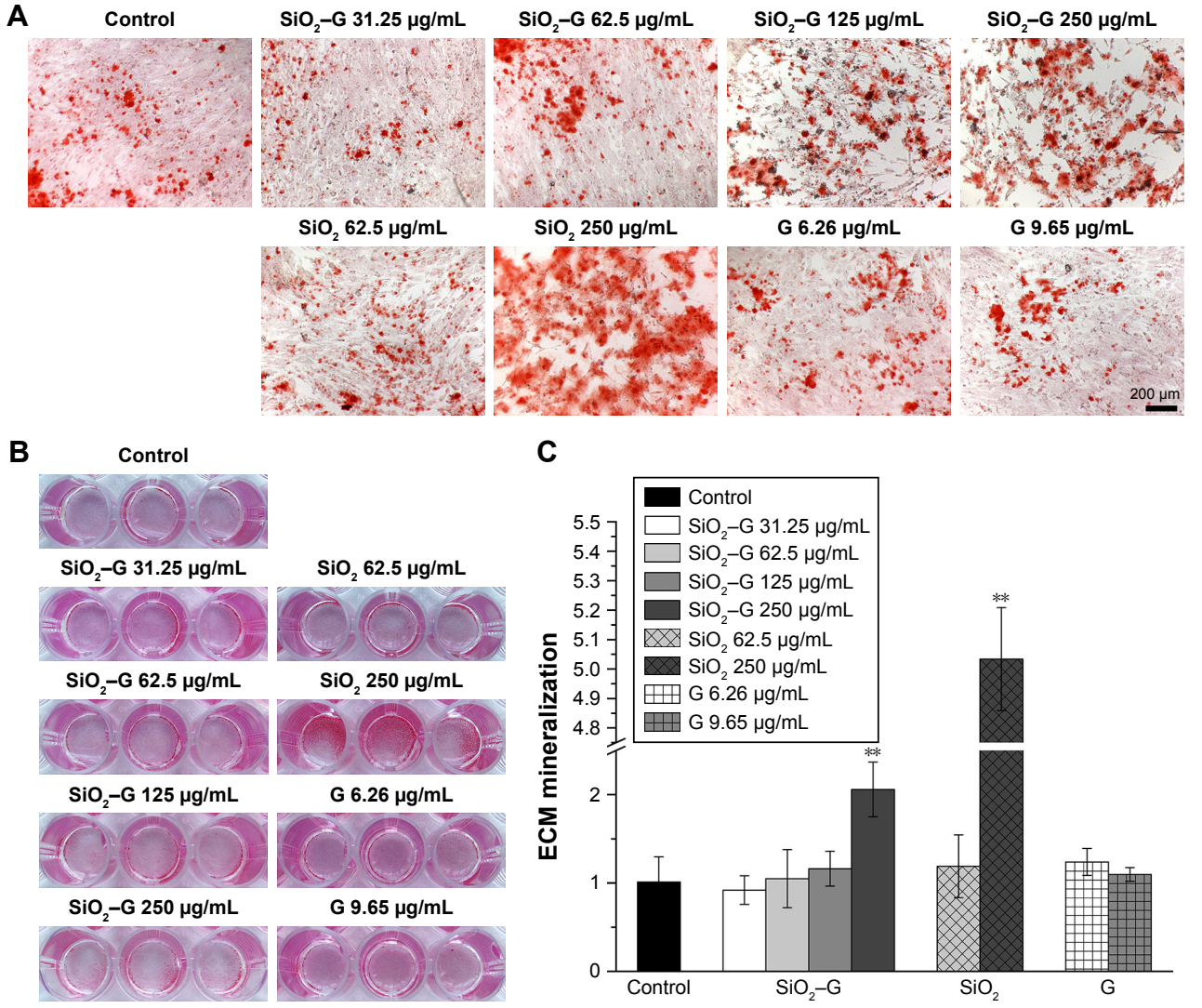

Figure 9 ECM mineralization of the SaOS-2 cells.
Notes: (**A**) Optical microscopic images and (**B**) macrograph of Alizarin Red S staining for matrix mineralization of cells after osteogenic induction for 14 days. (**C**) The quantitative results of retention of Alizarin Red S. Data are expressed as mean ± SD (n=3 for each sample). $^{**}p<0.01$ compared with the control group.
Abbreviations: ECM, extracellular matrix; SiO_2, silica; SiO_2–G, SiO_2–gentamicin nanohybrids; G, gentamicin.

ion is cytotoxic at high concentrations.[36] Thus, the concentration of Si ions in the cell culture medium was analyzed by inductively coupled plasma mass spectrometry (ICP-MS). Figure S1 depicts that SiO_2–gentamicin nanohybrids released much less Si ions than that of the SiO_2 NPs at each time point during the incubation, implicating that the higher toxicity of the SiO_2–gentamicin nanohybrids than that of the native SiO_2 NPs may not be attributed to the release of Si ions. Moreover, previous studies have shown that increasing the concentrations of silicate caused a higher growth rate of SaOS-2 cells and the maximal stimulation occurs at 1,000 μM (28 μg/mL concentration of Si ions).[37,38] Therefore, the released Si ions from the SiO_2–gentamicin nanohybrids should not contribute to the cytotoxicity. Further work should be done to clarify the possible mechanism for the higher cytotoxicity of the SiO_2–gentamicin nanohybrids.

In our previous study, the minimum inhibitory concentration (MIC) of the SiO_2–gentamicin nanohybrids against *Bacillus subtilis*, *Pseudomonas fluorescens* and *Escherichia coli* was 250 μg/mL. The concentration of released gentamicin from the 250 μg/mL SiO_2–gentamicin nanohybrids after immersion for 24 and 72 h was 6.26 and 9.65 μg/mL, respectively.[21] Therefore, a concentration of 250 μg/mL for the SiO_2–gentamicin nanohybrids was tested and the experimental concentration of free gentamicin was set as 6.26 and 9.65 μg/mL (since the medium was changed every 3 days) in the present study. Moreover, after exposure of the cells to the NPs tested, both the SiO_2–gentamicin nanohybrids

and native SiO_2 NPs show partial aggregation on the surface of the cells (Figure S2). The aggregation remained in the wells even though the medium was frequently changed. Therefore, the remaining SiO_2–gentamicin nanohybrids in the wells would continuously release gentamicin during the incubation for 2–3 weeks. The present results show that both SiO_2–gentamicin nanohybrids and native SiO_2 NPs at a high concentration (250 μg/mL) decrease the expression of ALP in SaOS-2 cells. On the other hand, the free gentamicin does not influence the ALP expression of the cells (Figure 6). The SiO_2–gentamicin nanohybrids consist of two compositions, SiO_2 NPs and gentamicin. Thus, it is assumed that the effect of SiO_2–gentamicin nanohybrids on osteogenesis of SaOS-2 cells is attributed to the SiO_2 NPs. ALP is an early expressed protein during osteogenic differentiation. A previous study has also reported that native SiO_2 NPs inhibited the ALP activity of BMSCs of rats.[28] Since both SiO_2–gentamicin nanohybrids and native SiO_2 NPs induce severe cytotoxicity to the SaOS-2 cells (Figure 4B) under osteogenic induction, consequently, the decreased ALP activity of SaOS-2 cells can be attributed to the severe toxicity induced by SiO_2–gentamicin nanohybrids and native SiO_2 NPs exposure.

The expression of COLI, OPN, and OCN is not influenced by the SiO_2–gentamicin nanohybrids and SiO_2 NPs, even in the high concentrations tested (Figure 8). The differentiation of osteoblasts to osteocytes is regulated by a group of specific molecules. RUNX2 is an initial marker exclusively expressed in mineralized tissues.[39] It causes a stage-dependent expression of osteogenesis-related markers, including ALP, COLI, OCN, and OPN; asialoprotein (ASP); and bone sialoprotein (BSP).[40] It has been suggested that COLI induces calcification of the stromal cell matrix.[41] OPN is a structural protein highly phosphorylated and glycosylated and is synthesized by preosteoblasts, osteoblasts, and osteocytes.[42] OCN is the most abundant bone-specific non-collagenous protein synthesized by osteoblasts and serves as a marker to evaluate osteogenic maturation and bone formation.[43] The presence of these proteins provides the basis for the upcoming mineralization, which is usually considered as a functional in vitro endpoint reflecting mature cell differentiation.[44]

In the present study, inconsistent results were found for the osteogenesis of SaOS-2 cells after exposure to SiO_2–gentamicin nanohybrids and native SiO_2 NPs. Both of the two materials tested at a high concentration (250 μg/mL) induce a lower expression of ALP but an enhanced ECM mineralization for the SaOS-2 cells. To ensure a better understanding of whether mineralization is cell mediated or driven by the presence of aggregates (nanohybrids or NPs) remaining throughout the culture time, a control experiment was conducted, in which the nanohybrids or NPs at a concentration of 250 μg/mL (in the absence of cells) were incubated in the same conditions as the culture. Alizarin Red S staining on day 14 showed that the SiO_2–gentamicin nanohybrids and native SiO_2 NPs were negative for the staining (Figure S3), implying that mineralization is mediated by the SaOS-2 cells, not by the aggregates (nanohybrids or NPs). A previous review has indicated that ALP activity is necessary, but not sufficient, to produce mineralized matrix.[44] Evans et al[45] have found that BMSCs of hypophysectomized rats expressed high levels of ALP activity, while producing few mineralization nodules, in comparison with BMSCs of non-hypophysectomized rats. Hence, it is evident that BMSCs can produce high levels of ALP in vitro even without mineralization. In another two studies, ECM mineralization was observed in human BMSCs that achieved a minimal ALP activity (~0.25 nmol/min/μg protein or 1.2 nmol/min/10,000 cells) during the culture period of 2–3 weeks.[46,47] From these aforementioned studies, it was observed that the levels of ALP activity were not in proportion to the observed mineralization levels. In the present study, the cells can still express low levels of ALP after exposure to a high concentration of SiO_2–gentamicin nanohybrids or native SiO_2 NPs (Figure 6). Thus, the above-mentioned reports support the present data that the cells achieve high levels of mineralization.

Previous studies have reported that SiO_2 NPs could promote the mineralization of both osteoclasts[13–15] and BMSCs.[12,13,16] SiO_2 NPs have also accelerated osteogenic differentiation of MC3T3-E1 cells as demonstrated by a more rapid increase in ALP activity and increased mineralization.[13,14] Similarly, it was revealed that the presence of SiO_2 NPs triggered upregulation of ALP/RUNX2 transcripts, bone-related matrix protein deposition (OCN and OPN), followed by matrix mineralization in mouse and human BMSCs.[12,13] Several possible mechanisms have been proposed for the positive effects of SiO_2 NPs on osteogenic differentiation of bone-related cells. Huang et al[17] have suggested that the internalization of SiO_2 NPs induced actin polymerization and activated the small GTP-bound protein RhoA, which then induced transient osteogenic signals in human BMSCs. Ha et al[14] have found that SiO_2 NPs promoted mineralization and differentiation of osteoblasts through stimulating ERK1/2 signaling pathway, which is necessary for the processing of LC3β-I to LC3β-II and activating autophagosome assembly. After internalization of SiO_2 NPs into the cells, they could be degraded and may

release Si ions.[16] Si ions at a given concentration significantly enhanced the proliferation, mineralization nodule formation, bone-related gene expression, and WNT and SHH signaling pathways of human BMSCs.[36] Consequently, it has emerged from these previous results that the possible mechanisms for enhanced osteogenesis induced by SiO_2 NPs are very complicated and more investigation should be conducted to elucidate them.

In the present study, both the SiO_2–gentamicin nanohybrids and native SiO_2 NPs decrease the cell viability of SaOS-2 cells even at a low exposure concentration (31.25 μg/mL). With regard to osteogenesis, SiO_2–gentamicin nanohybrids and native SiO_2 NPs at a concentration range of 31.25–125 μg/mL do not influence the osteogenic differentiation capacity of SaOS-2 cells, while at a high concentration (250 μg/mL), the two materials tested induce a lower expression of ALP but an enhanced ECM mineralization. Up to now, a considerable number of researchers have paid attention to the potential cytotoxicity of SiO_2 NPs, and some of this published literature[9–11] has claimed that SiO_2 NPs were cytotoxic to different cell lines. Therefore, caution should be exercised when SiO_2–gentamicin nanohybrids or native SiO_2 NPs are used in orthopedics. Moreover, this study shows that free gentamicin at concentrations of 6.26 and 9.65 μg/mL does not influence the cell viability and osteogenic differentiation capacity of SaOS-2 cells, providing some suggestions for the safe use of gentamicin, at considerable concentrations (6.26–9.65 μg/mL), in orthopedic applications.

Conclusion

In the present study, we have explored the effects of SiO_2–gentamicin nanohybrids on the osteogenic differentiation of human osteoblast-like cells, together with native SiO_2 NPs and free gentamicin. The cells were exposed to the synthesized SiO_2–gentamicin nanohybrids at a concentration range of 31.25–125 μg/mL for 72 h. The results show that both SiO_2–gentamicin nanohybrids and native SiO_2 NPs decrease the cell viability of SaOS-2 cells in a time- and dose-dependent manner. SiO_2–gentamicin nanohybrids and native SiO_2 NPs at a concentration range of 31.25–125 μg/mL do not influence the osteogenic differentiation capacity of SaOS-2 cells. However, a high concentration (250 μg/mL) of the two materials tested induce a lower expression of ALP but an enhanced ECM mineralization. Free gentamicin (6.26 and 9.65 μg/mL) does not significantly influence the cell viability and osteogenic differentiation capacity of SaOS-2 cells. We suggest that further investigation on the effects of SiO_2–gentamicin nanohybrids on the behaviors of stem cells or other regular osteoblasts should be conducted to make a full evaluation of the safety of SiO_2–gentamicin nanohybrids in orthopedic applications.

Acknowledgments

The authors would like to acknowledge the financial support from National Natural Science Foundation of China (31700829, 51472139, 51473019), Fundamental Research Funds for the Central Universities (FRF-TP-16-034A1) and China Postdoctoral Science Foundation (2017M620610).

Disclosure

The authors report no conflicts of interest in this work.

References

1. Park MV, Verharen HW, Zwart E, et al. Genotoxicity evaluation of amorphous silica nanoparticles of different sizes using the micronucleus and the plasmid lacZ gene mutation assay. *Nanotoxicology*. 2011; 5(2):168–181.
2. Qian J, Wang D, Cai F, Zhan Q, Wang Y, He S. Photosensitizer encapsulated organically modified silica nanoparticles for direct two-photon photodynamic therapy and in vivo functional imaging. *Biomaterials*. 2012;33(19):4851–4860.
3. Li Z, Barnes JC, Bosoy A, Stoddart JF, Zink JI. Mesoporous silica nanoparticles in biomedical applications. *Chem Soc Rev*. 2012;41(7): 2590–2605.
4. Lee JE, Lee N, Kim T, Kim J, Hyeon T. Multifunctional mesoporous silica nanocomposite nanoparticles for theranostic applications. *Acc Chem Res*. 2011;44(10):893–902.
5. Agnihotri S, Pathak R, Jha D, et al. Synthesis and antimicrobial activity of aminoglycoside-conjugated silica nanoparticles against clinical and resistant bacteria. *New J Chem*. 2015;39(9):6746–6755.
6. Faber C, Stallmann HP, Lyaruu D, et al. Comparable efficacies of the antimicrobial peptide human lactoferrin 1-11 and gentamicin in a chronic methicillin-resistant *Staphylococcus aureus* osteomyelitis model. *Antimicrob Agents Chemother*. 2005;49(6):2438–2444.
7. Shi X, Wang Y, Ren L, Zhao N, Gong Y, Wang D-A. Novel mesoporous silica-based antibiotic releasing scaffold for bone repair. *Acta Biomater*. 2009;5(5):1697–1707.
8. Xue J, Shi M. PLGA/mesoporous silica hybrid structure for controlled drug release. *J Control Release*. 2004;98(2):209–217.
9. Lu X, Qian J, Zhou H, et al. In vitro cytotoxicity and induction of apoptosis by silica nanoparticles in human HepG2 hepatoma cells. *Int J Nanomedicine*. 2011;6:1889–1901.
10. Duan J, Yu Y, Li Y, Yu Y, Sun Z. Cardiovascular toxicity evaluation of silica nanoparticles in endothelial cells and zebrafish model. *Biomaterials*. 2013;34(23):5853–5862.
11. Kim I-Y, Joachim E, Choi H, Kim K. Toxicity of silica nanoparticles depends on size, dose, and cell type. *Nanomedicine*. 2015;11(6): 1407–1416.
12. Gaharwar AK, Mihaila SM, Swami A, et al. Bioactive silicate nanoplatelets for osteogenic differentiation of human mesenchymal stem cells. *Adv Mater Deerfield*. 2013;25(24):3329–3336.
13. Ha S-W, Sikorski JA, Weitzmann MN, Beck GR. Bio-active engineered 50 nm silica nanoparticles with bone anabolic activity: therapeutic index, effective concentration, and cytotoxicity profile in vitro. *Toxicol In Vitro*. 2014;28(3):354–364.
14. Ha S-W, Weitzmann MN, Beck GR Jr. Bioactive silica nanoparticles promote osteoblast differentiation through stimulation of autophagy and direct association with LC3 and p62. *ACS Nano*. 2014;8(6): 5898–5910.

15. Beck GR, Ha S-W, Camalier CE, et al. Bioactive silica-based nanoparticles stimulate bone-forming osteoblasts, suppress bone-resorbing osteoclasts, and enhance bone mineral density in vivo. *Nanomedicine*. 2012;8(6):793–803.
16. Yang X, Li Y, Liu X, et al. The stimulatory effect of silica nanoparticles on osteogenic differentiation of human mesenchymal stem cells. *Biomed Mater*. 2016;12(1):015001.
17. Huang D-M, Chung T-H, Hung Y, et al. Internalization of mesoporous silica nanoparticles induces transient but not sufficient osteogenic signals in human mesenchymal stem cells. *Toxicol Appl Pharmacol*. 2008;231(2):208–215.
18. Huang D-M, Hung Y, Ko B-S, et al. Highly efficient cellular labeling of mesoporous nanoparticles in human mesenchymal stem cells: implication for stem cell tracking. *FASEB J*. 2005;19(14):2014–2016.
19. Ince A, Schütze N, Karl N, Löhr JF, Eulert J. Gentamicin negatively influenced osteogenic function in vitro. *Int Orthop*. 2007;31(2):223–228.
20. Kagiwada H, Fukuchi T, Machida H, Yamashita K, Ohgushi H. Effect of gentamicin on growth and differentiation of human mesenchymal stem cells. *J Toxicol Pathol*. 2008;21(1):61–67.
21. Mosselhy DA, Ge Y, Gasik M, Nordström K, Natri O, Hannula S-P. Silica-gentamicin nanohybrids: synthesis and antimicrobial action. *Materials (Basel)*. 2016;9(3):170.
22. Corrêa GG, Morais E, Brambilla R, et al. Effects of the sol–gel route on the structural characteristics and antibacterial activity of silica-encapsulated gentamicin. *Colloids Surf B Biointerfaces*. 2014;116:510–517.
23. Thomas CR, George S, Horst AM, et al. Nanomaterials in the environment: from materials to high-throughput screening to organisms. *ACS Nano*. 2011;5(1):13–20.
24. He W, Kienzle A, Liu X, Müller WE, Elkhooly TA, Feng Q. In vitro effect of 30 nm silver nanoparticles on adipogenic differentiation of human mesenchymal stem cells. *J Biomed Nanotechnol*. 2016;12(3):525–535.
25. He W, Elkhooly TA, Liu X, et al. Silver nanoparticle based coatings enhance adipogenesis compared to osteogenesis in human mesenchymal stem cells through oxidative stress. *J Mater Chem B*. 2016;4(8):1466–1479.
26. Van de Belt H, Neut D, Uges D, et al. Surface roughness, porosity and wettability of gentamicin-loaded bone cements and their antibiotic release. *Biomaterials*. 2000;21(19):1981–1987.
27. Stallmann HP, Faber C, Bronckers AL, Amerongen AVN, Wuisman PI. In vitro gentamicin release from commercially available calcium-phosphate bone substitutes influence of carrier type on duration of the release profile. *BMC Musculoskelet Disord*. 2006;7(1):18.
28. Zhou X, Feng W, Qiu K, et al. BMP-2 derived peptide and dexamethasone incorporated mesoporous silica nanoparticles for enhanced osteogenic differentiation of bone mesenchymal stem cells. *ACS Appl Mater Interfaces*. 2015;7(29):15777–15789.
29. Sahoo B, Devi KSP, Sahu SK, et al. Facile preparation of multifunctional hollow silica nanoparticles and their cancer specific targeting effect. *Biomater Sci*. 2013;1(6):647–657.
30. Sharma S, Bano S, Ghosh AS, et al. Silk fibroin nanoparticles support in vitro sustained antibiotic release and osteogenesis on titanium surface. *Nanomedicine*. 2016;12(5):1193–1204.
31. Sarabia-Sainz A, Montfort GR-C, Lizardi-Mendoza J, et al. Formulation and characterization of gentamicin-loaded albumin microspheres as a potential drug carrier for the treatment of *E. coli* K88 infections. *Int J Drug Deliv*. 2012;4(2):209.
32. Pandey H, Parashar V, Parashar R, Prakash R, Ramteke PW, Pandey AC. Controlled drug release characteristics and enhanced antibacterial effect of graphene nanosheets containing gentamicin sulfate. *Nanoscale*. 2011;3(10):4104–4108.
33. Perni S, Prokopovich P. Continuous release of gentamicin from gold nanocarriers. *RSC Adv*. 2014;4(94):51904–51910.
34. Vivero-Escoto JL, Slowing II, Lin VS-Y. Tuning the cellular uptake and cytotoxicity properties of oligonucleotide intercalator-functionalized mesoporous silica nanoparticles with human cervical cancer cells HeLa. *Biomaterials*. 2010;31(6):1325–1333.
35. Huang X, Teng X, Chen D, Tang F, He J. The effect of the shape of mesoporous silica nanoparticles on cellular uptake and cell function. *Biomaterials*. 2010;31(3):438–448.
36. Han P, Wu C, Xiao Y. The effect of silicate ions on proliferation, osteogenic differentiation and cell signalling pathways (WNT and SHH) of bone marrow stromal cells. *Biomater Sci*. 2013;1(4):379–392.
37. Wiens M, Wang X, Schröder HC, et al. The role of biosilica in the osteoprotegerin/RANKL ratio in human osteoblast-like cells. *Biomaterials*. 2010;31(30):7716–7725.
38. Schröder HC, Wang XH, Wiens M, et al. Silicate modulates the cross-talk between osteoblasts (SaOS-2) and osteoclasts (RAW 264.7 cells): inhibition of osteoclast growth and differentiation. *J Cell Biochem*. 2012;113(10):3197–3206.
39. Ducy P, Schinke T, Karsenty G. The osteoblast: a sophisticated fibroblast under central surveillance. *Science*. 2000;289(5484):1501–1504.
40. Wang X, Schröder HC, Wiens M, Ushijima H, Müller WE. Bio-silica and bio-polyphosphate: applications in biomedicine (bone formation). *Curr Opin Biotechnol*. 2012;23(4):570–578.
41. Mizuno M, Kuboki Y. Osteoblast-related gene expression of bone marrow cells during the osteoblastic differentiation induced by type I collagen. *J Biochem*. 2001;129(1):133–138.
42. Butler WT. The nature and significance of osteopontin. *Connect Tissue Res*. 1989;23(2–3):123–136.
43. Ducy P, Desbois C, Boyce B, et al. Increased bone formation in osteocalcin-deficient mice. *Nature*. 1996;382(6590):448–452.
44. Hoemann C, El-Gabalawy H, McKee M. In vitro osteogenesis assays: influence of the primary cell source on alkaline phosphatase activity and mineralization. *Pathol Biol (Paris)*. 2009;57(4):318–323.
45. Evans JF, Yeh JK, Aloia JF. Osteoblast-like cells of the hypophysectomized rat: a model of aberrant osteoblast development. *Am J Physiol Endocrinol Metab*. 2000;278(5):E832–E838.
46. Fromigue O, Marie P, Lomri A. Bone morphogenetic protein-2 and transforming growth factor-b2 interact to modulate human bone marrow stromal cell proliferation and differentiation. *J Cell Biochem*. 1998;68(4):411–426.
47. Chang P-L, Blair HC, Zhao X, et al. Comparison of fetal and adult marrow stromal cells in osteogenesis with and without glucocorticoids. *Connect Tissue Res*. 2006;47(2):67–76.

Supplementary materials

Materials and methods

Concentration of Si ions in the cell culture medium for the silica (SiO_2)–gentamicin nanohybrids and native SiO_2 nanoparticles (NPs)

Before the experiments, the NPs were exposed to ^{60}Co irradiation at a dose of 10 kGy for sterilization. The samples were added to the cell culture plate in the same way as in the cell culture experiments. In brief, SiO_2–gentamicin nanohybrids and native SiO_2 NPs were first suspended in the osteogenic induction medium to a concentration of 1 mg/mL and ultrasonically vibrated for 1 h. Then, the medium containing nanohybrids or NPs was diluted to 250 μg/mL and added to the cell culture plate. The samples were kept in a 5% CO_2 humidified incubator at 37°C, and the medium was refreshed every 3 days. On days 3, 6, 9, 12, and 15, the medium containing the released Si ions was collected, centrifuged, and then, the supernatants were analyzed by inductively coupled plasma mass spectrometry (ICP-MS; Agilent 7500ce; Agilent Technologies, Santa Clara, CA, USA).

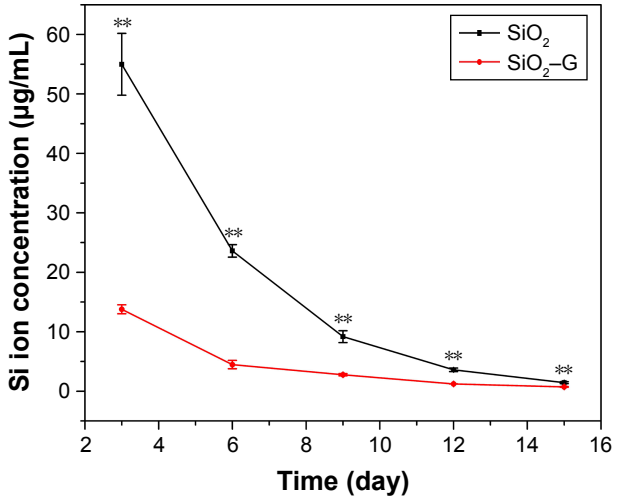

Figure S1 Concentration of Si ions for the samples incubated in the cell culture medium.

Notes: The SiO_2–gentamicin nanohybrids and native SiO_2 NPs at a concentration of 250 μg/mL were incubated in osteogenic induction medium. On days 3, 6, 9, 12, and 15, the medium containing the released Si ions was collected and then analyzed by ICP-MS. $^{**}p<0.01$ compared with the SiO_2 NPs.

Abbreviations: SiO_2, silica; SiO_2–G, SiO_2–gentamicin nanohybrids; G, gentamicin; NPs, nanoparticles; ICP-MS, inductively coupled plasma mass spectrometry.

Results

Concentration of Si ions in the cell culture medium for the SiO_2–gentamicin nanohybrids and native SiO_2 NPs

Figure S1 depicts the concentrations of Si ions released from the SiO_2–gentamicin nanohybrids and native SiO_2 NPs on days 3, 6, 9, 12, and 15 after incubation. For the SiO_2 NPs (250 μg/mL), concentrations of Si ions in the cell culture medium were 54.986±5.202, 23.605±1.043, 9.177±1.001, 3.591±0.293, and 1.441±0.164 μg/mL, respectively. The concentrations of Si ions released from the SiO_2–gentamicin nanohybrids in the cell culture medium at each time point were 13.776±0.746, 4.474±0.700, 2.768±0.190, 1.228±0.007, and 0.715±0.059 μg/mL, respectively. SiO_2–gentamicin nanohybrids released much less Si ions than the SiO_2 NPs. The reason for this slower release may be attributed to the loaded gentamicin on the surfaces of the SiO_2–gentamicin nanohybrids (as shown in Figure 1B), limiting the release of the Si ions. Similar results have been shown in a recent study by Choi and Kim,[1] verifying that drug-loaded mesoporous SiO_2 NPs show a relatively slower release of Si ions than the free mesoporous SiO_2 NPs at the initial degradation stage.

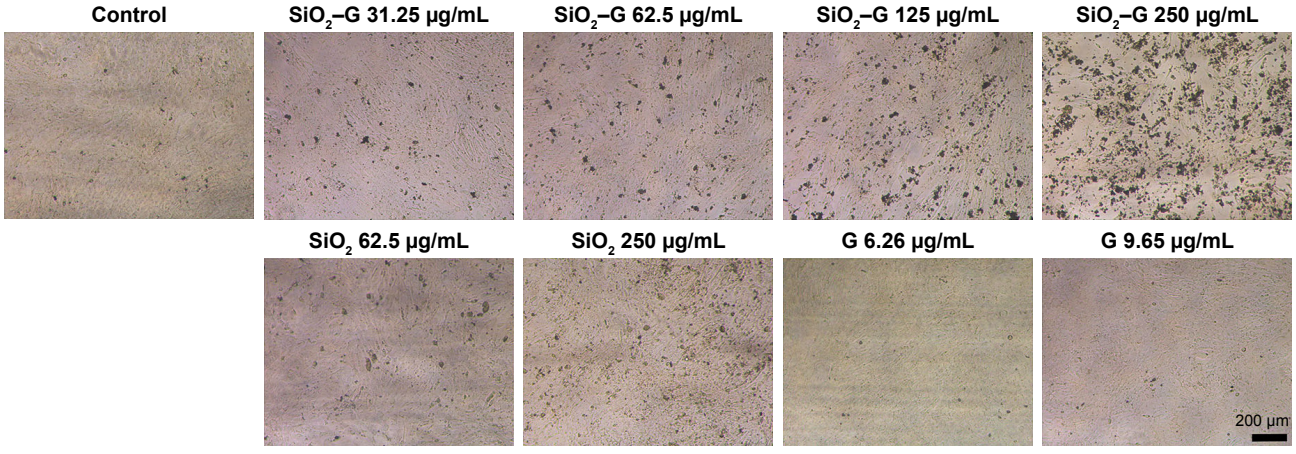

Figure S2 Optical microscopic images of cells.

Notes: The cells were incubated with different concentrations of SiO_2–G nanohybrids, SiO_2 NPs, and G for 24 h in the osteogenic induction medium.

Abbreviations: SiO_2, silica; SiO_2–G, SiO_2–gentamicin nanohybrids; G, gentamicin; NPs, nanoparticles.

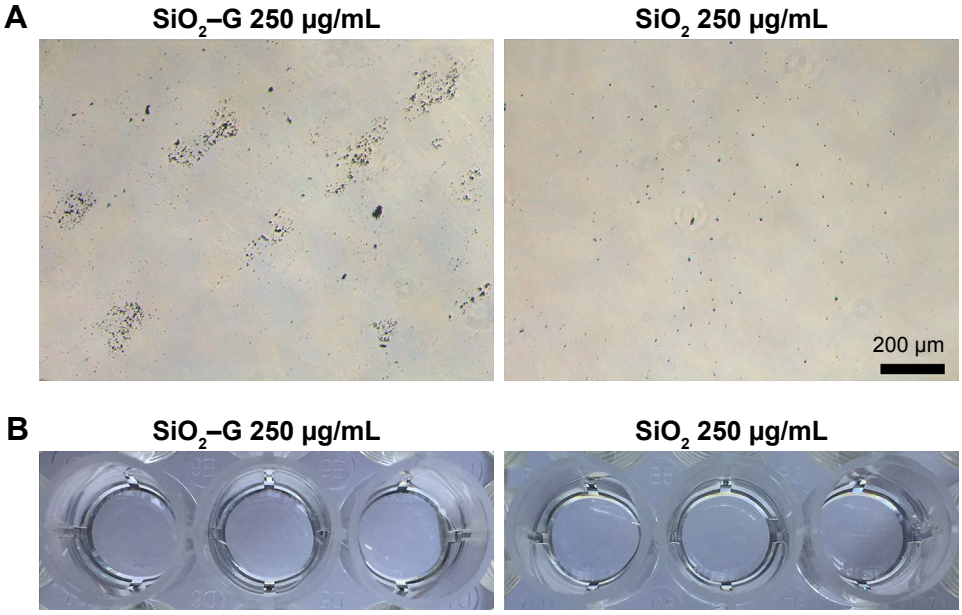

Figure S3 Mineralization of the SiO_2–G and SiO_2 NPs.
Notes: (**A**) Optical microscopic images and (**B**) macrograph of Alizarin Red S staining for mineralization of SiO_2–G nanohybrids and SiO_2 NPs at a concentration of 250 µg/mL (in the absence of cells) after osteogenic induction for 14 days.
Abbreviations: SiO_2, silica; SiO_2–G, SiO_2–gentamicin nanohybrids; G, gentamicin; NPs, nanoparticles.

Reference

1. Choi E, Kim S. How can doxorubicin loading orchestrate in vitro degradation behaviors of mesoporous silica nanoparticles under a physiological condition? *Langmuir*. 2017;33(20):4974–4980.